SUPPORTING INFORMATION FOR

Effects of methacrylic acid and pendant vinyl groups on the mechanical properties of highly stretchable core-shell nanostructured films deposited from water

James Turton*[a], Stephen Worrall[b], Muhamad S. Musa[c], Amir H. Milani[a,*], Yichao Yao[a], Peter Shaw[c], David Ring[c] and Brian R. Saunders[a,*]

[a] *Department of Materials, MSS Tower, The University of Manchester, Manchester, M1 3BB, U.K.* [b] *Aston Institute of Materials Research, School of Engineering and Applied Science, Aston University, Birmingham, B4 7ET, U.K.* [c] *Synthomer (UK) Ltd, Temple Fields, Harlow, Essex, CM20 2BH, U.K.*

Vinyl functionalisation of the particles via ring-opening epoxide reaction

Scheme S1A shows the overall vinyl-functionalisation reaction with one of the possible products. The reaction mechanism shown in Scheme S1B is based on that reported by Reis et al.[1] The first step is the transfer of a proton to glycidyl methacrylate (GMA). Then, ring-opening by the OH group occurs by nucleophilic attack at the A and / or B carbons. This results in two possible isomers, which are both shown. Reis et al. were not able to determine which of the isomers is more favourable. The carbon labelled A is less sterically hindered and would seem more likely to react. Consequently, we depict the isomer from path A in this work. We note that the isomer from path B may also be present.

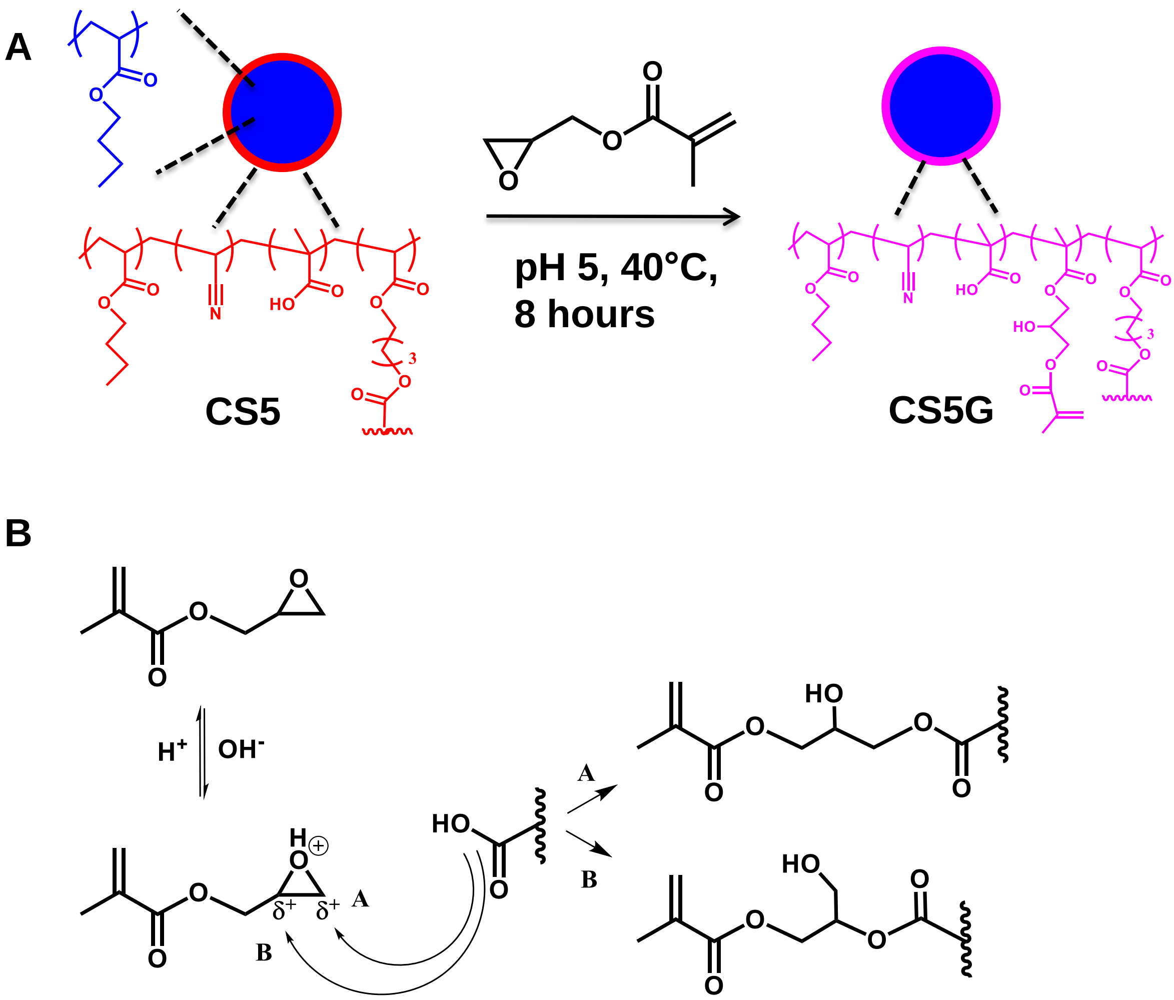

Scheme S1. A. Depiction of the method used for the GMA functionalisation of CS5 nanoparticles to prepare CS5G nanoparticles. **B.** Mechanism for epoxide ring-opening reaction.

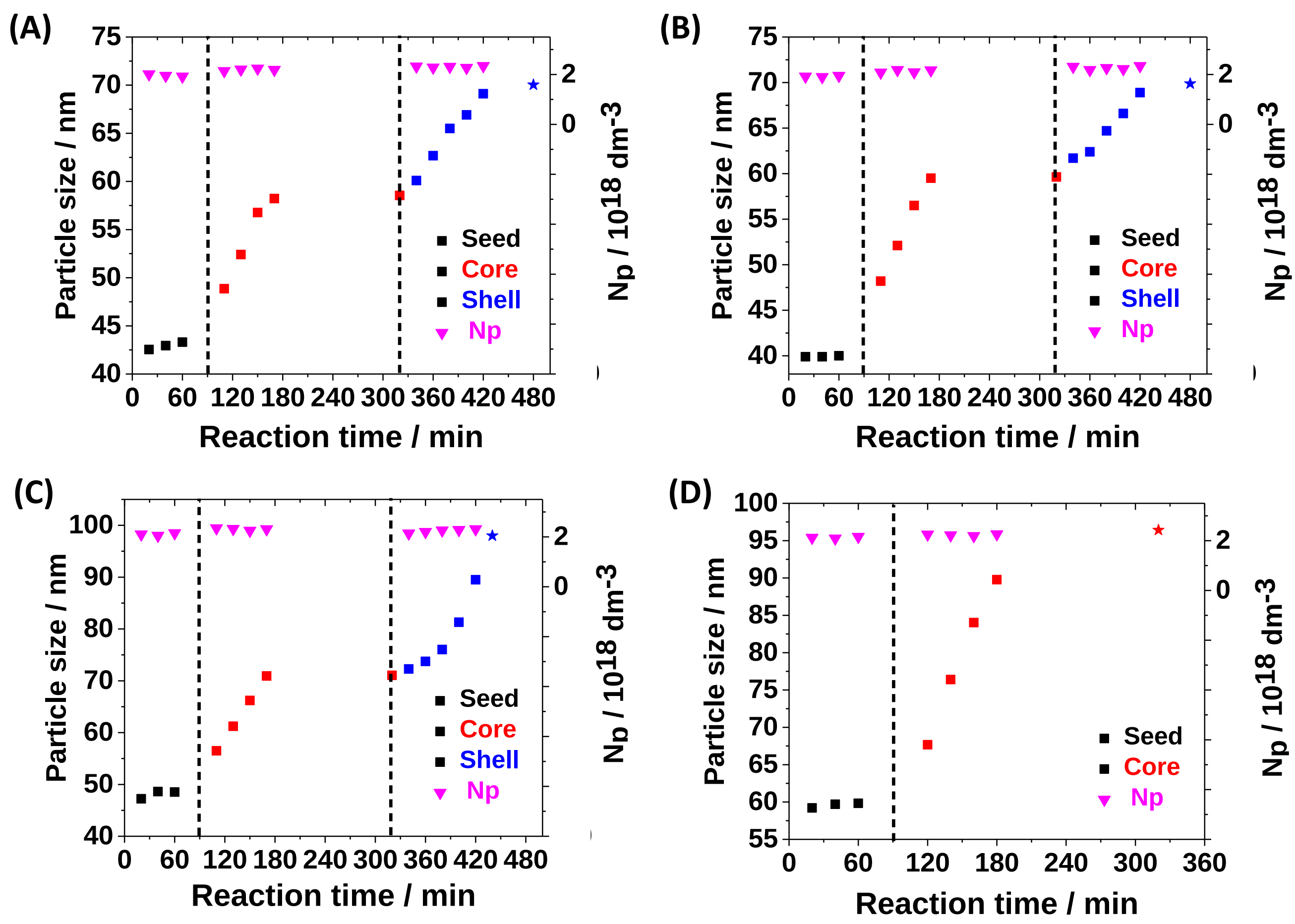

Fig. S1. z-average particle size and number density of particles (N_p) versus preparation time for (**A**) CS0, (**B**) CS2.5, (**C**) CS10 core-shell and **(D)** NP5 systems. The stars show the final *d* values.

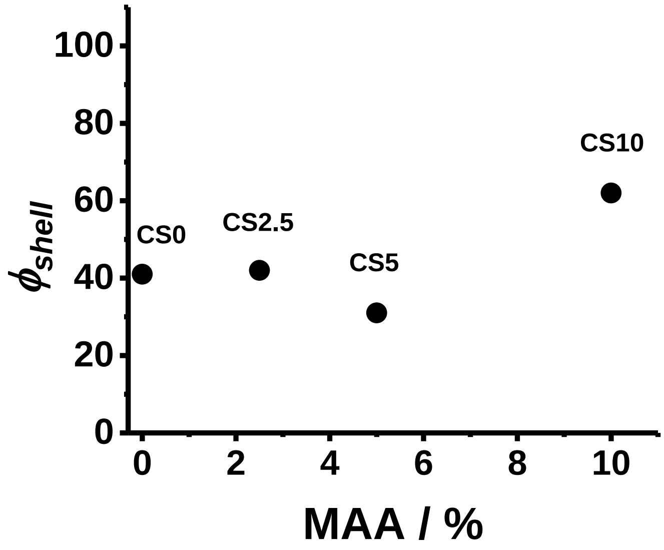

Fig. S2. Variation of shell volume fraction with MAA content used during preparation. The identities of the nanoparticles are shown.

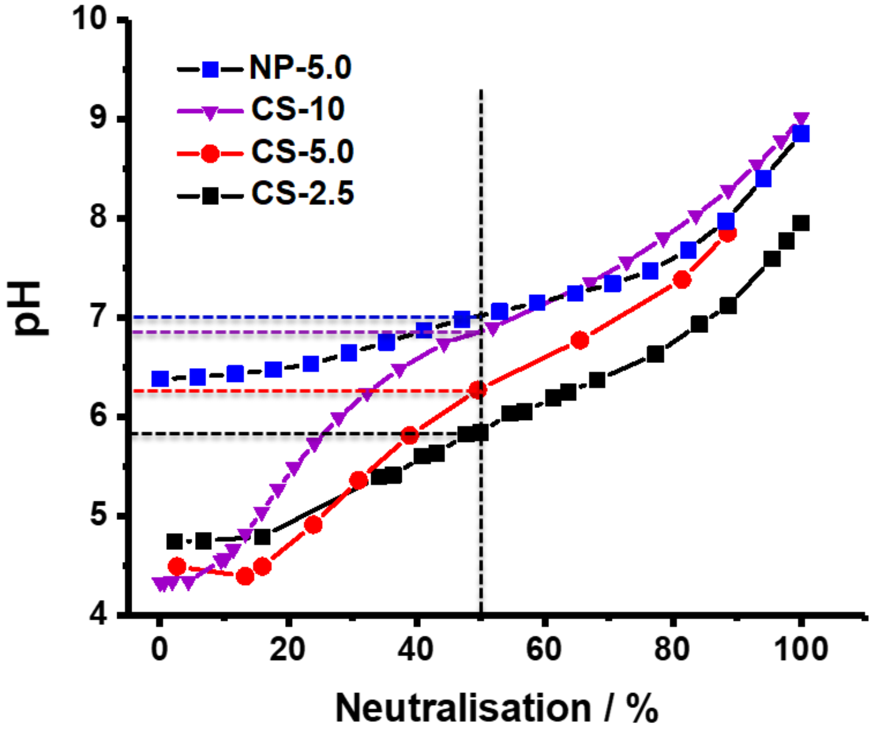

Fig. S3. Potentiometric titration data for various nanoparticle dispersions. The apparent pK_a values were determined from the pH values at 50 % neutralisation which is represented by the dotted lines.

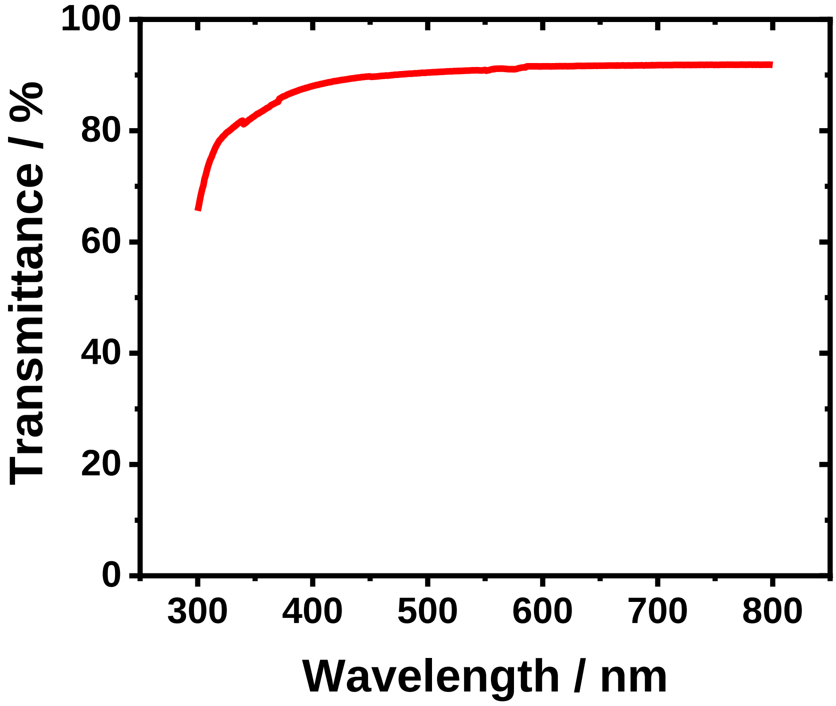

Fig. S4. Transmittance versus wavelength for the CS5 film shown in Scheme 1A.

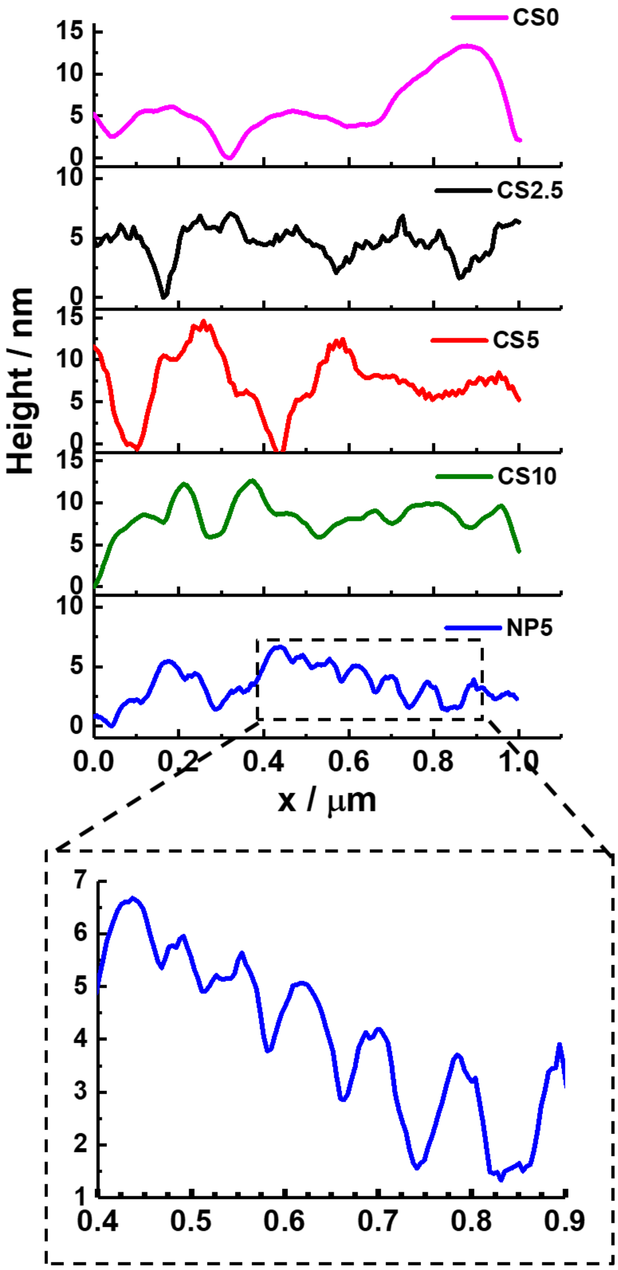

Fig. S5. Line profiles from height mode AFM images in Fig. 3 for various films.

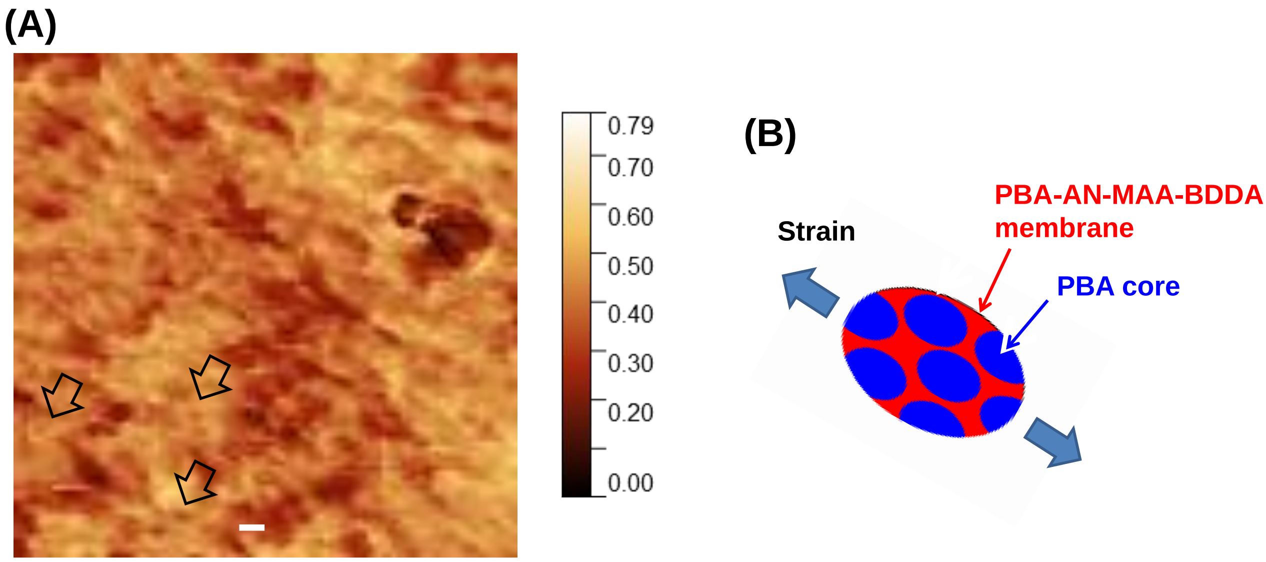

Fig. S6. (A) AFM log stiffness image for the CS10 film. The black arrows highlight the membrane morphology. The shells are elongated in a preferred direction indicating that the film had been subjected to unintentional strain during processing. Scale bar: 200 nm. **(B)** Depiction of a segment of film showing the strained polymer cores within the membrane formed from inter-meshed shells.

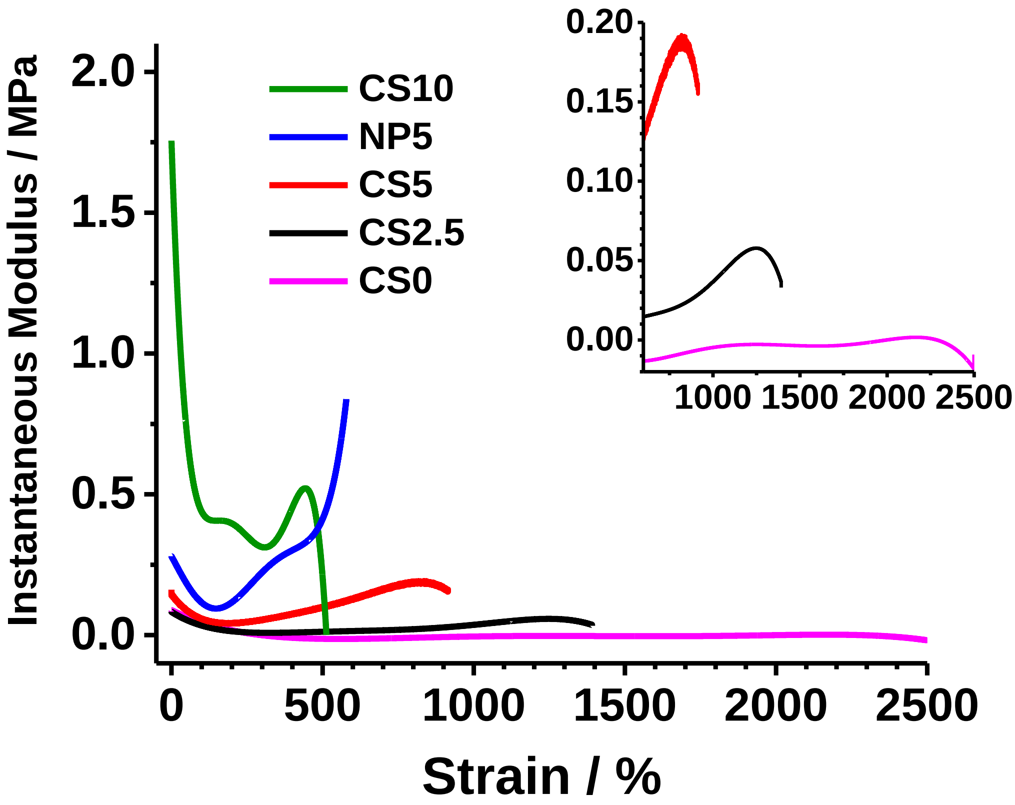

Fig. S7. Instantaneous modulus (or tangent modulus) values obtained from the data shown in Fig. 5A. These values were calculated using the local gradients of the stress-strain data.

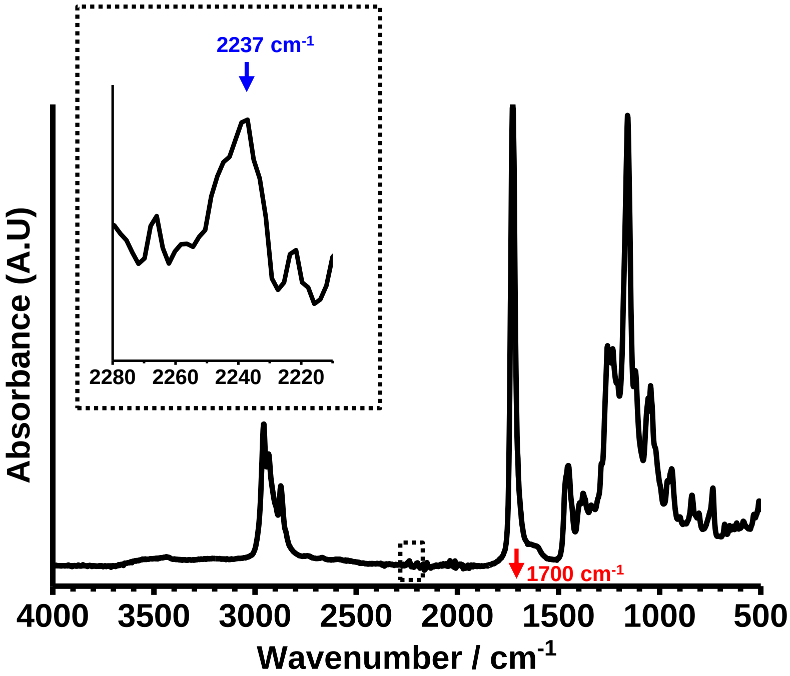

Fig. S8. FTIR spectrum of the CS5 film. Bonds due to -C≡N and hydrogen bonded -C=O groups are expected at 2237 and 1700 cm $^{-1}$, respectively. See text in the main paper for discussion.

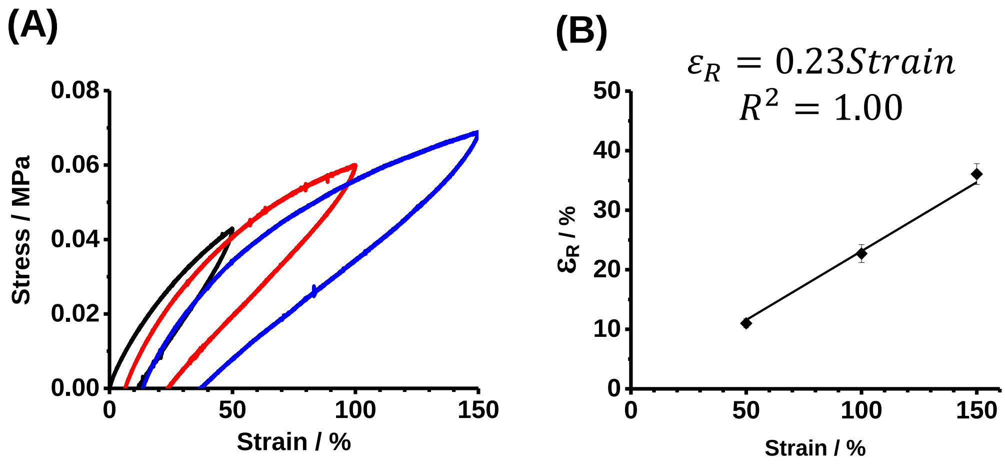

Fig. S9. (A) Dynamic tensile stress-strain data and **(B)** Residual strain vs. strain from (A) for CS5 films.

(A)

(B)

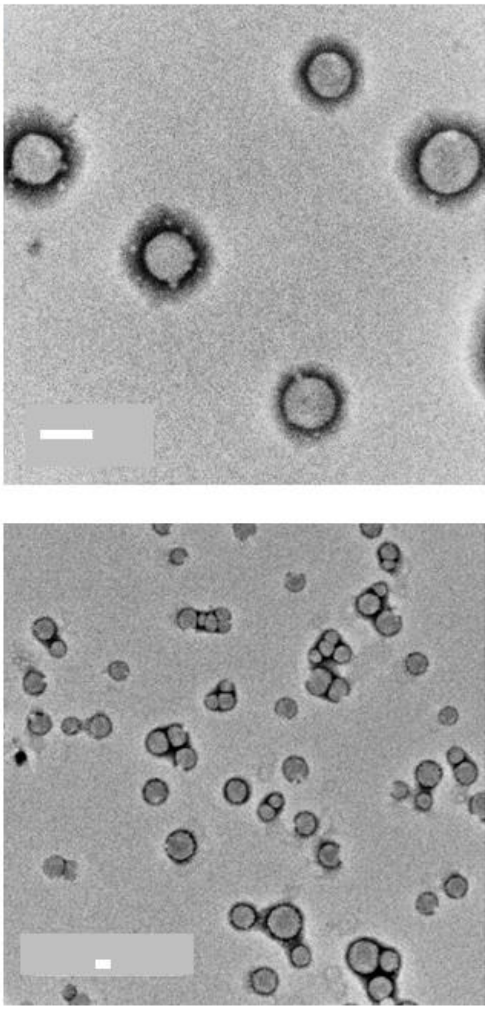

Fig. S10. TEM data for CS5G particles. Higher and lower magnification images are shown in **(A)** and **(B)**, respectively. The scale bars are 100 nm

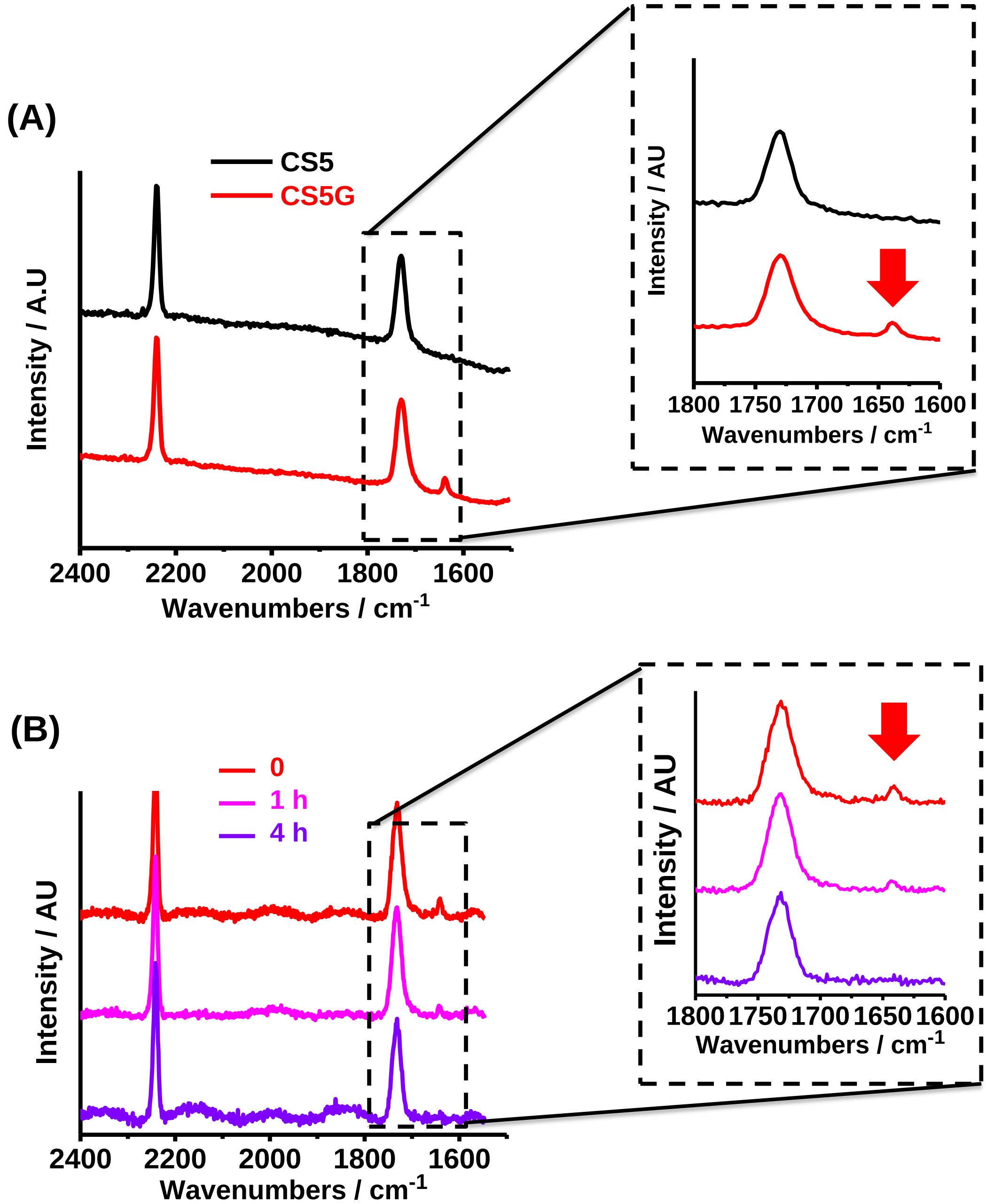

Fig. S11. (A) Raman spectra showing both CS5 and CS5G films. A vinyl peak is evident (arrow). **(B)** Raman spectra for a CS5G film before and after heating at 90 °C for 1 and 4 h. The vinyl peak disappears due to crosslinking when the film is heated for 4 h.

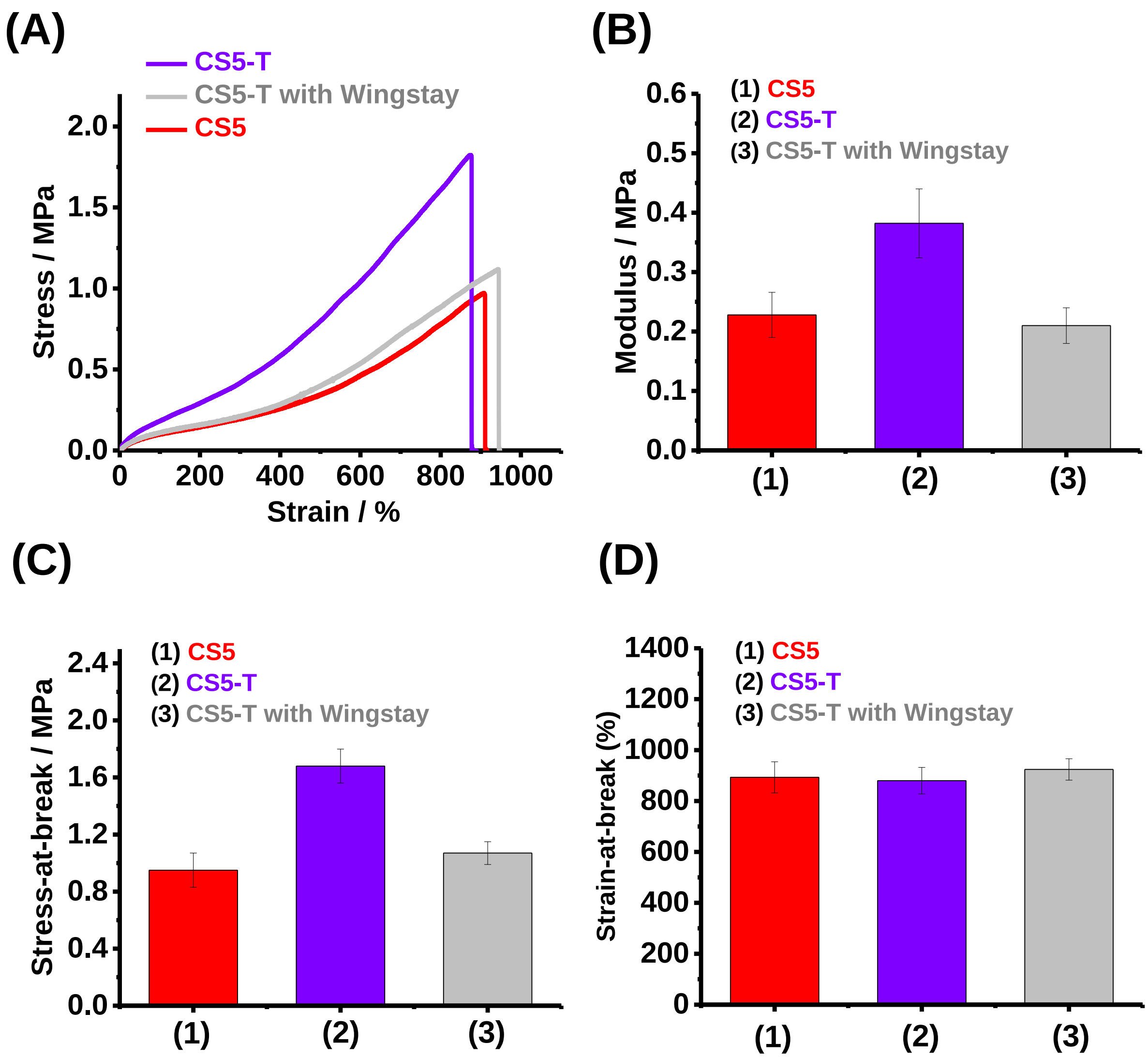

Fig. S12. (A) Stress/strain curves for CS5 films heated at 90 °C for 4 h (denoted as CS5-T) and with added Wingstay-L. The effects of heating in the absence and presence of Wingstay-L on the **(B)** modulus, **(C)** stress-at-break and **(D)** strain-at-break are shown.

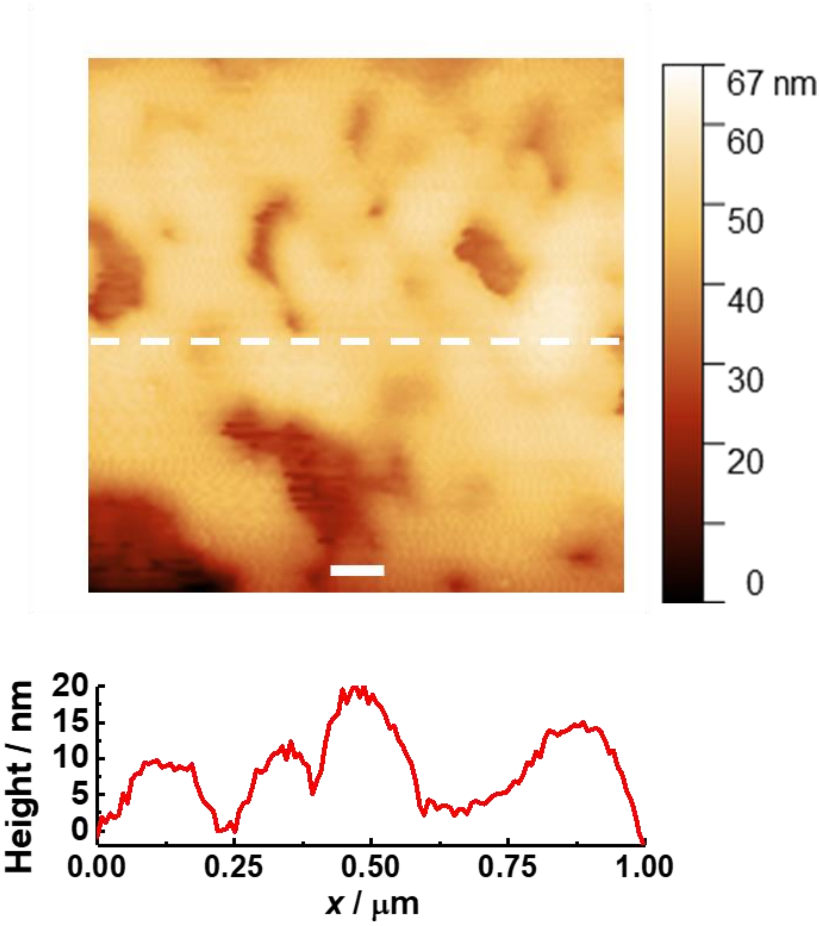

Fig. S13. AFM height image and line profile for CS5G film. The scale bar is 100 nm.

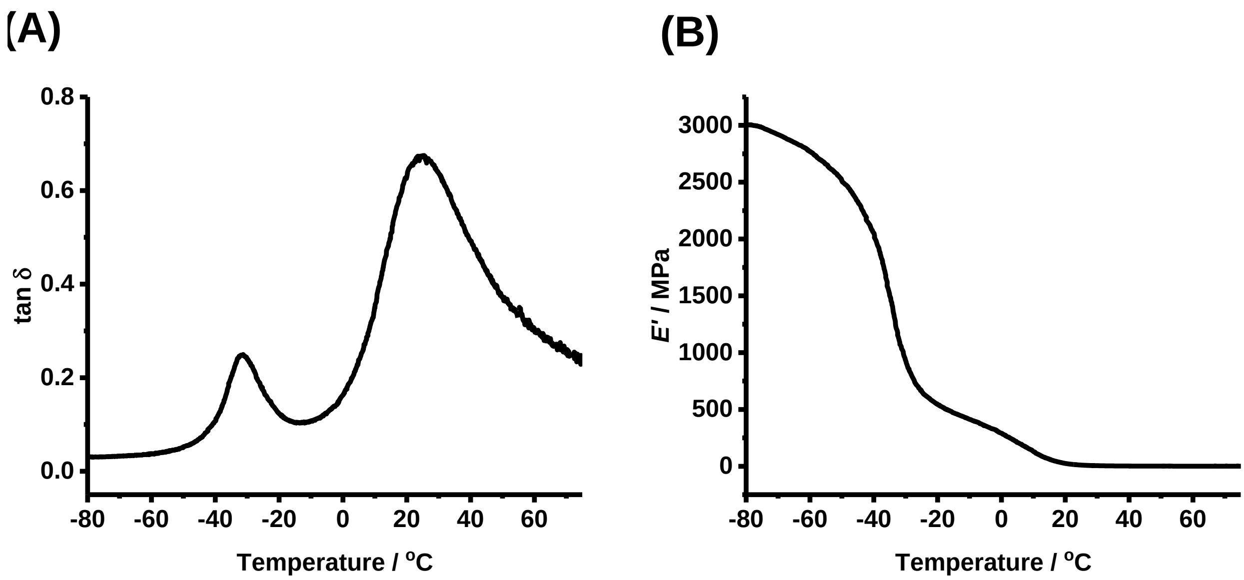

Fig. S14. Temperature-dependent **(A)** tan δ (= *E"*/*E'*, where *E"* and *E'* are the loss and storage modulus, respectively) and **(B)** *E'* values for a CS5G film.

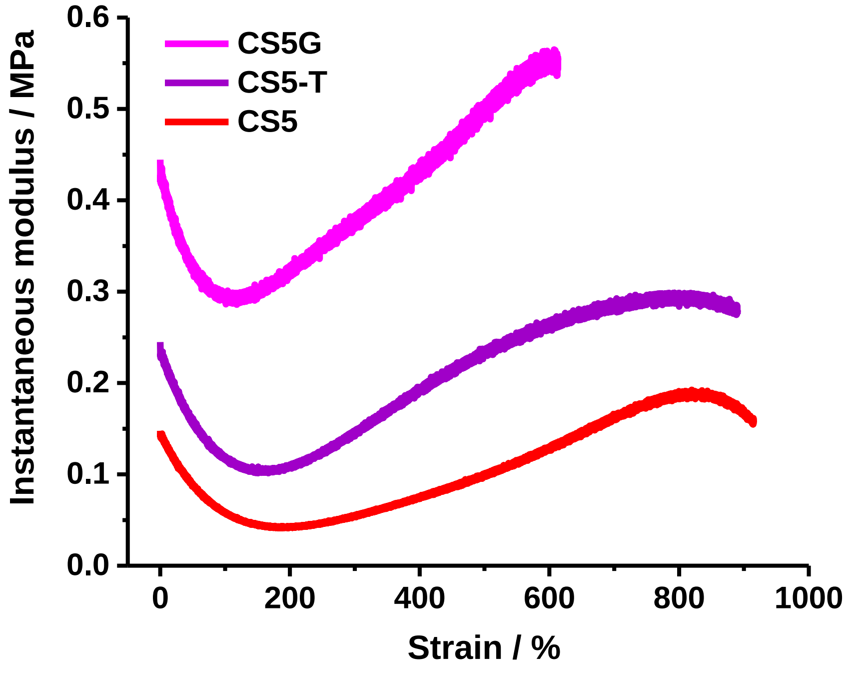

Fig. S15. Instantaneous modulus as a function of strain for CS5G, CS5-T and CS5 films. The data were obtained from Fig. 7A and Fig. 5A.

Table S1. Monomer masses used to prepare the CSx nanoparticles

	Seed	Core	Shell			
System	**BA mass / g**	**BA mass / g**	**BA mass / g**	**AN mass / g**	**MAA mass / g**	**BDDA mass / g**
CS0	13.5	59.38	43.94	11.88	-	0.60
CS2.5	13.5	59.38	43.94	11.88	1.49	0.60
CS5.0	13.5	59.38	43.94	11.88	2.98	0.60
CS10	13.5	59.38	43.94	11.88	5.96	0.60

Table S2. Properties of non-functionalised CSx nanoparticles

System	$W_{MAA(th)}$ [a]/ wt%	$W_{MAA(exp)}$ [b]/ wt%	pK_a [c]	D_{TEM} [d] /nm [CV]	d_c [e] / nm	d_{c-s} [f] / nm	δ [g] / nm	ϕ_{shell} [h] / vol.%
CS0	-	-	-	74 [9]	58	69	5.5	41
CS2.5	1.3	1.4	5.9	76 [11]	60	72	6	42
CS5	2.5	2.4	6.3	78 [10]	75	85	5	31
CS10	5.0	4.7	6.9	91 [11]	71	98	13.5	62
NP5	5.0	6.6	7.0	98 [10]	60 [i]	96 [i]	-	100

[a] Theoretical particle MAA content determined from the preparation conditions employed. [b] MAA content determined by potentiometric titration. [c] Apparent pK_a value which was taken from the titration data at 50% neutralisation. [d] Number-average particle diameter from TEM. CV is the coefficient of variation. [e] z-average diameter obtained from DLS data for the core particles. [f] z-average diameter obtained from DLS data for the core-shell particles. [g] Shell thickness = $(d_{c-s} - d_c)/2$. [h] Shell volume fraction = $1 - \{(d_c/d_{c-s})\}^3$. [i] The NP5 system is considered homogeneous. These values for d_c and d_{c-s} correspond to the d values after the first and second stages of growth from Fig. S1D.

References

1. A. V. Reis, A. R. Fajardo, I. T. A. Schuquel, M. R. Guilherme, G. J. Vidotti, A. F. Rubira and E. C. Muniz, *J. Org. Chem.*, 2009, **74**, 3750-3757.